Behaviors of geogrid-reinforced ballasted railway under train loads

Qiusheng Gu[1], X. Bian[1], S. He[2], and D. Gong[2]

[1] Dept. of Civil Engineering, Key Laboratory of Soft Soils and Geoenvironmental Engineering, MOE, Zhejiang University, Hangzhou 310058, China.
[2] Tensar Corporation China, Wuhan, 430056, China

ABSTRACT

Ballast is a layer of aggregate particles with specific gradation to support track structure. Ballast layer plays an essential role in distributing the train loadings from the track structure to underlying subgrade soil. This paper presents the experimental results of triaxial tests on ballast materials with and without geogrid reinforcement with various confining pressure. Axial strain, conferential strain and volumetric strain are recorded during the test. These tests indicated that the installation of geogrid depresses the development of lateral and volumetric deformation, and effectively increases the peak deviator stress values of the ballast specimen. Visual check of the deformation of geogrid after test shows that the breakage of the geogrid is aggravated with the increase of confining pressure.

Keywords: Ballast; triaxial test; Geogrid reinforcement

1 INTRODUCTION

The track substructure of a modern ballasted railway usually consists of a ballast bed, a subballast layer, and subgrade soil, as the sectional view shown in Fig.1. It plays an essential role in distributing the loads from the track superstructure (rails and sleepers) uniformly and providing lateral resistance as well. With the rapid development of railway transportation system, the speed and load of trains are constantly increasing, the stronger loading intensity will accelerate track deterioration (Bian et al.2014) consequently, which primarily occurs in the ballast layer. Seed et al. (1962) verified that the maximum vertical contact stress beneath the sleeper base of railseats should be 200 kPa to 270 kPa under a 200kN wheel load. Raymond and Raymond and Davies(1978) demonstrated that the axial stresses at sleeper/ballast interfaces could hardly exceed 140 kPa under a static axle load of 150 kN. In practice, the axial and lateral stress that develop within ballast layer are related to the axle train load, the initial degree of compaction and the restraint provided by the sleepers. B. Indraratna et al. (1998) compared the effects of different confining pressures on the triaxial tests of ballast and found that the deformation and shear strength of ballast under confining pressures are quite different. Aingaran, S. (2014) conducted both dry and saturated tests of ballast materials based on the large triaxial test and found that the "stick-slip" phenomenon will lead to a non-smooth deviator stress curve. The deviator stress eventually reaches a peak and starts to drop slightly showing strain softening behaviour.

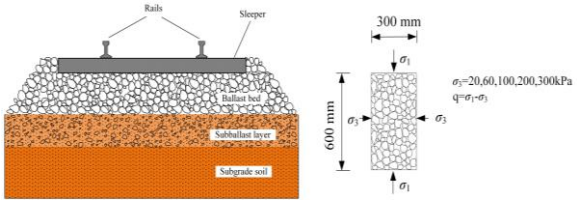

Fig. 1. Ballasted railway and ballast loading condition

Geogrids have been utilized to reinforce ballast layer to reduce track settlement and improve lateral stability successfully. However, most of the previous studies (Bathurst and Raymond, 1987; Raymond and Ismail, 2003; Indraratna et al., 2006) only considered the deformation performance of ballast layer, few of them comprehensively explored the performance and reinforcement mechanism of reinforced ballast layer. Qian et al.(2015) studied the reinforcement effect of geogrids on well-graded ballast specimens and deteriorated ballast specimens by means of large triaxial tests. It was found that geogrids can significantly increase the peak deviator stress of ballast specimens.

In order to study the reinforcement effect of geogrids on ballast materials, triaxial tests of ballast specimens with and without geogrid were investigated based on large-diameter triaxial testing apparatus (LDTTA) in this study. Specimens of 300 mm (diameter) by 600 mm (height), 92% compactness degree and follow the gradation of Chinese first level ballast standard. In order to explore the reinforcement effect and mechanism of geogrids, deviator stress, confining pressure, volumetric deformation and circumferential strain in the middle of the ballast specimen were monitored during the whole test

process.

2 EXPERIMENTAL PROCEDURES

2.1 Test apparatus

As shown in Fig.2, the DSY-300 large-diameter triaxial testing apparatus (LDTTA) of Zhejiang University utilized in this study consists of six main parts: the triaxial chamber, axial loading device, confining pressure boosting system, servo oil sources, loading control system, and corresponding data acquisition system. The axial load and confining pressure were applied to the specimen by an axial loading device and a confining pressure–boosting system respectively. A load cell and several confining pressure sensors were installed to monitor the stresses exerted on the specimen. The LDTTA adopted an electro-hydraulic servo program with a closed-loop control system to ensure the loading process accurate and stable. The axial strain of the specimen was calculated by the linear variable differential transformer (LVDT) installed at the top of the specimen, and the variation of the specimen's volume would be measured by of water volume in the triaxial chamber.

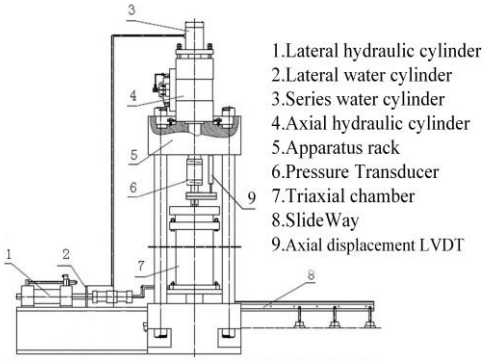

Fig. 2. Large-diameter cyclic triaxial testing apparatus.

2.2 Specimen preparation

The ballast materials adopted in this study are tuff that taken from a railway construction site near Hangzhou. The grain size distribution (as shown in Fig.3) followed the requirements of the Chinese first-level railway ballast standard. The mechanical behaviors of granular materials strongly depend on compaction and the compaction of the ballast materials is defined as the ratio of the actual density to the maximum dry density. The maximum dry density of the tuff sample is 1642.67kg/m³ and the corresponding porosity ratio is 0.545. Therefore, the packing density of a 92% compaction degree of the specimens in this study is 1511.26kg/m³ and the corresponding porosity ratio is 0.679. The geogrid used in the study is TriAx® TX150L provided by Tensar International Corporation. The properties contributing to the performance of geogrid as a mechanically stabilized layer include the following Table 1 and Table 2.

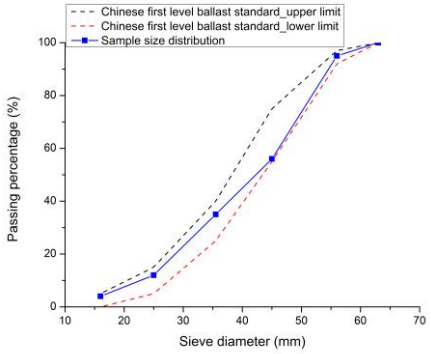

Fig. 3. Grain-size distribution of ballast materials.

Table 1. Shape properties of TX150L geogrid.

Index Properties	Longitudinal	Diagonal	General
Rib pitch(mm)	57	57	
Rib shape			Rectangular
Aperture shape			Triangular

Table 2. Structural properties of TX150L geogrid.

Structural Integrity	General
Junction efficiency(%)	93
Isotropic Stiffness Ratio	0.6
Overall Flexural Rigidity(mg-cm)	750000
Radial stiffness at low strain(kN/m @ 0.5% strain)	325

Each ballast was poured into an iron split mold in four lifts, and each lift was compacted with hammer carefully. After compaction of the first two lifts, one layer of geogrid was placed carefully in the middle of the test specimen for making a geogrid reinforced ballast sample. A rubber pad (4 mm thick) was used to minimize the risk of breaking sharp corners and edges during compaction. The mean bulk packing density of the compacted specimens was determined to be around 1511.26kg/m³. Two 2.5-mm-thick rubber membranes were used to confine the cylindrical specimens and avoid being puncturing by sharp corners and edges of ballast during test. Bishop and Henkel (1962)has proved that even thin rubber membranes can provide some confinement which increase the measured principal stresses. B. Indraratna(1998) proved rubber membranes with pressures higher than 120kPa, the membrane corrections amounted to less than 2% of the measured principal stresses, whereas at the lowest confining pressure 1kPa, the maximum correction was below 8%. Hence, the confinement provided by the rubber membranes has little effect on the data interpretation and the final conclusions.

2.3 Applied monotonic loading in triaxial tests

Five confining pressures (20kPa, 60kPa, 100kPa, 200kPa and 300kPa) were adopted in this study. By comparing and analyzing the test results under various confining pressures, the effects of geogrid reinforcement on the performance of ballast specimens were studied. The confining pressure remains stable

during the test. The axial loading is controlled by displacement and the shearing rate is 5mm/min. When the axial strain reaches 15%, the specimen is considered to fail and the loading process ended.

3 EXPERIMENTAL RESULTS OF TRIAXIAL TESTS

3.1 Deviator stress and volumetric strain

Cylindrical specimens were used in triaxial test. The specimen is subjected to the same circumferential pressure in three axes through the pressurized liquid in the pressure chamber and the whole test process remains unchanged. The specimen is then subjected to vertical axial pressure through the piston until the specimen is sheared. During the loading process of ballast specimens by actuators, the axial strain of the specimens and the variation of the axial load of the specimens are monitored through the vertical axial load sensor and the LVDT on the top. Fig.4 presents stress state from large-scale triaxial shear strength tests conducted on the ballast specimens for up to 15% axial strain. Under the same confining pressure, the deviator stress of the specimens strengthened with geogrid is significantly greater than that of the specimens without geogrid at the same axial strain. The increase of deviator stress of the geogrid reinforced specimens is mainly due to the lateral restraint provided by the geogrid. At the same time, with the increase of confining pressure, the deviator stress can be significantly increased.

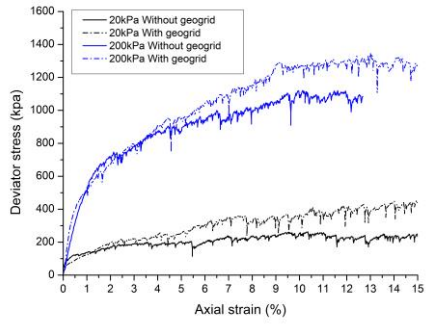

Fig. 4. Deviator stress–axial strain response under different confining pressure

During the loading process of the tests, the volume change of ballast specimen were monitored through the volume change of confining water at the end of confining cylinder. Fig. 5 shows the volumetric deformation of the specimens in tests. Under low confining pressure, the specimens always dilates during the shear process, and the growth of specimen's volume were limited by geogrid. Under high confining pressure, the volume of the sample increases first and then decreases, while the radial expansion in the middle of the sample is always limited by the geogrid.

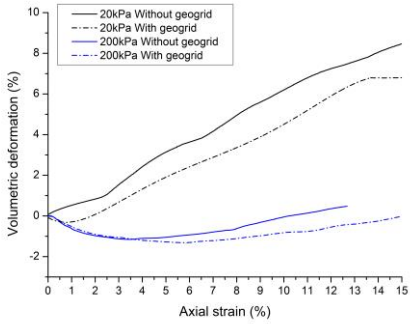

Fig. 5. Volumetric deformation–axial strain response under various confining pressure.

3.2 Circumferential strain

The circumferential strain of the middle part of the ballast sample is monitored through a wire-drawn displacement sensor arranged in the middle part of the ballast sample. Fig. 6 shows the circumferential strain of the specimens in this test. The circumferential strain in the middle of the specimen increases continuously in all the tests, and the geogrid will restrict the radial expansion of the specimen. Under high confining pressure, the confinement effect of geogrid on the circumferential strain in the middle of the specimen is less significant than that under low confining pressure. At the same time, under different confining pressure conditions, the higher the confining pressure, the smaller the circumferential strain of the ballast specimen, and the later the restriction of geogrid on the circumferential strain of the specimen is exerted, and the less significant the effect is.

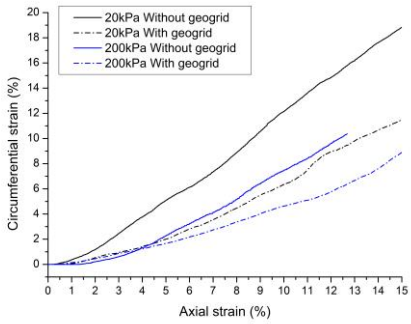

Fig. 6. Circumferential strain–axial strain response under different confining pressure.

3.3 Geogrid breakage

After the test, the geogrids were taken out for comparative analysis. Fig. 7 shows the stress state of the specimens in this test, in which the deviating stress is included. The reinforcing effect of geogrids on ballast specimens is mainly due to restraining the lateral deformation of ballast specimens. With the increase of

the axial strain during the test, the geogrid in the middle of the sample will eventually be destroyed. Under low confining pressure, the ribs at the edge of the grille only fragmented slightly, and most of the area of the geogrid was intact. Under high confining pressure, the ribs at the edge of the geogrid were seriously broken, and almost all the ribs near the central area were broken. According to the experimental results, it can be found that with the increase of confining pressure, the breakage of the geogrid increases.

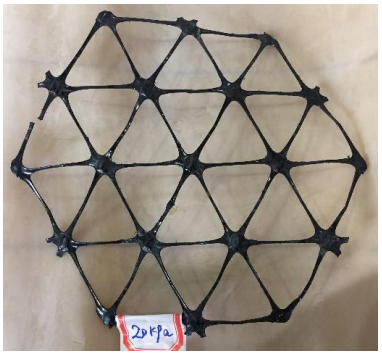

(a) confining pressure 20kPa

(b) confining pressure 200kPa

Fig. 7. Geogrid breakage under different confining pressure.

4 CONCLUSION

Triaxial test of ballast with and without geogrid reinforcement were carried out with various confining pressures. The data of deviator stress, volume deformation, circumferential strain and volumetric strain of ballast specimens were recorded and analyzed during the loading process to study the effects of geogrid reinforcement on ballast. The main conclusions are as follows:

(1) Test results indicated that installation of geogrid in the ballast can increase the bearing capacity of ballast material, this performance improvement mainly attributes to the constrain of ballast particle movements in lateral direction by the presence of geogrid. At the same time, with the increase of confining pressure, the strength of the ballast can be significantly increased.

(2) The circumferential strain in the middle of the specimen increases all the time during the tests, and the geogrid installation limits the radial expansion of the specimen. Geogrid shows stronger constrain on ballast's lateral deformation when the confining pressure is lower.

(3) Because of the radial expansion in the middle of the specimen during the loading process, the effect of geogrid on the volumetric deformation of the specimen is mainly due to the restriction of the radial expansion. Geogrid installation reduces volumetric dilation when the confining pressure is low, while facilitates volumetric reduction when the confining pressure is high.

(4) With the increase of confining pressure, the breakage of the geogrid is aggravated.

REFERENCES

Bian, X. C., Jiang, H. G., Cheng, C., Chen, Y.M., Chen, R. P., and Jiang, J. J.(2014). Full-scale model testing on a ballastless high-speed railway under simulated train moving loads. J. Soil Dyn. Earthquake Eng., 66, 368–384.

Seed, H., Chan, C., Lee, C., TRANSPORTATION, I. O. & ENGINEERING, T. (1962). Resilience characteristics of subgrade soils and their relation to fatigue failures in asphalt pavements.

Raymond, G. P., and Davies, J. R. (1978). Triaxial test on dolomite railroad ballast. J. Soil Mech. and Found. Div., ASCE, 104(6).737751.

Indraratna, B.; Ionescu, D.; and Christie, H. D(1998). Shear Behaviour of Railway Ballast based on Large Scale Triaxial Testing. Journal of Geotechnical and Geoenvironmental Engineering/ Volume 124 Issue 5.

Aingaran, S. (2014) Experimental investigation of static and cyclic behavior of scaled railway ballast and the effect of stress reversal. PhD thesis, University of Southampton

Bathurst, R.J., Raymond, G.P., (1987). Geogrid reinforcement of ballasted track. Transp. Res. Rec. 1153, 8e14.

Brown, S.F., Kwan, J., Thom, N.H., (2007). Identifying the key parameters that influence geogrid reinforcement of railway ballast. Geotext. Geomembr. 25(6), 326e335.

Indraratna, B., Khabbaz, H., Salim, W., Christie, D., (2006). Geotechnical properties of ballast and the role of geosynthetics in rail track stabilization. J. Ground Improv.10 (3), 91e102.

Qian, Y., Mishra, D., Tutumluer, E., and Kazmee, H. A. (2015). "Characterization of geogrid reinforced ballast behavior at different levels of degradation through triaxial shear strength test and discrete element modeling." Geotext. Geomembr., 43(5), 393–402.

Bishop, W. A., and Henkel, D. J. (1962). The measurement of soils properties in the triaxial test. Edward Arnold Ltd., London, U.K